PHYSICAL REVIEW B VOLUME 57, NUMBER 16 15 APRIL 1998-II

Self-ordering of quantum-wire superlattices on V-grooved substrates

Giorgio Biasiol, Eli Kapon, Yann Ducommun, and Anders Gustafsson*
Department of Physics, Swiss Federal Institute of Technology-EPFL, 1015 Lausanne, Switzerland
(Received 13 January 1998)

A mechanism of self-ordering of quantum-wire superlattices via growth on nonplanar substrates is described. Alternate deposition of thin layers characterized by a longer and a shorter diffusion length of adatoms on a self-limiting V groove yields an exact compensation of the increase and decrease in the surface curvature. As a result, a self-limiting surface profile develops, which gives rise to a vertically stacked superlattice (SL) of crescent-shaped quantum wires (QWR's). The structure of such SL's is accurately modeled using the self-limiting growth characteristics of thick layers of the barrier and well materials. A systematic difference, found between the average composition of these QWR SL's and the corresponding alloys, is interpreted in terms of the role of the entropy of mixing in the self-limiting growth process. [S0163-1829(98)51916-9]

Superlattices (SL's) of two-dimensional (2D) semiconductor heterostructures have been studied extensively, yielding insight into tunneling between 2D systems, the formation of SL minibands, localization of SL wave functions in the presence of disorder or electric fields, Bloch oscillations of electronic wave packets, and other phenomena.[1–5] The extension of these studies to SL's of lower-dimensional structures such as quantum wires (QWR's) and quantum dots (QD's) is expected to yield new interesting features due to the additional degrees of quantum confinement in these structures.

Whereas 2D SL structures are routinely produced at present by well-controlled thin-film growth techniques, the realization of QWR and QD SL's is much more difficult. Conventional lithography techniques are of limited use because of the stringent requirements on the interface quality and the physical separation of the wires and dots involved. On the other hand, several approaches relying on *self-ordering* phenomena have been explored recently for producing high-quality low-dimensional SL's. Growth of fractional-layer QWR SL's using vicinal substrates has been proposed and studied.[6,7] In this case, the lateral and vertical definition as well as the alignment of the wires rely on surface diffusion and preferential attachment of adatoms to the ledges of monolayer steps. The nonuniformities in such SL structures, resulting from imperfect step configuration and nonuniform growth rates, were partly rectified by resorting to growth of serpentine SL structures, in which the growth rate is intentionally varied during the deposition of the fractional layer SL on the vicinal substrate.[8] Similarly, a certain degree of lateral and vertical ordering has been observed in strained wire SL's formed on macrosteps during growth on misoriented substrates.[9] Strain-driven Stranski-Krastanow (SK) growth has been shown to yield vertically stacked QD columns for sufficiently thin barrier layers.[10–14] The vertical alignment of the dots in each column is achieved due to anisotropic surface diffusion of adatoms induced by the strain fields that are produced by the underlying dot layers.[10] A certain degree of lateral ordering of SK dots has been reported as well.[15,16] Strain effects have also been argued to play an important role in producing dense arrays of strained QWR's grown on (100) substrates.[17] Nonuniformities in these spontaneously formed SL structures, particularly due to vertical misalignment of the wires or dots, result from random fluctuations in the chemical potential that are greater than the ones inducing the vertical ordering.

Another self-ordering mechanism that has been utilized for growing highly uniform single and multiple semiconductor QWR's relies on organometallic chemical vapor deposition (OMCVD) of thin layers on V-grooved substrates.[18,19] In this case, a self-limiting surface profile is obtained due to the perfect equalization of the growth rate at nanofacets formed at the bottom of the groove.[20] A crescent-shaped QWR is then formed by depositing a thin layer of a lower band-gap semiconductor whose adatoms are characterized by a greater surface diffusion length. The position of the QWR is seeded by the position of the initial groove on the patterned substrate, and can thus lead to highly ordered wire arrays. Moreover, this self-ordering process can yield vertically stacked, virtually identical wires simply by repeatedly growing low band-gap wires separated by higher band-gap barriers.[21] However, to produce a wire of identical shape and size at each period of such multiple QWR structures it is necessary to fully recover the self-limiting surface profile during barrier growth.[22] The exponential recovery of the surface curvature[22] permits relatively thin barrier layers (>10 nm) for such recovery; however, the resulting wire separations are too large for observing significant QWR SL effects.

In the present paper we report on a self-ordering mechanism of vertical QWR superlattices, taking place during the growth of ultrathin layers on nonplanar substrates. The SL structure is grown on an $Al_xGa_{1-x}As$ V groove that exhibits a self-limiting surface profile. The growth of $GaAs/Al_xGa_{1-x}As$ SL structures with $Al_xGa_{1-x}As$ layers much thinner than the critical thickness required for full surface profile recovery does not allow the self-ordering of multiple QWR structures as described earlier. However, we find that after a short transient, an exact balance between the surface curvature increase and decrease during growth of the GaAs and the $Al_xGa_{1-x}As$ layers occurs, yielding a new self-limiting phase of a $GaAs/Al_xGa_{1-x}As$ QWR SL. We develop a model, based on the self-limiting surface evolution during growth of thick GaAs and $Al_xGa_{1-x}As$ layers in such V grooves, which quantitatively explains this growth mechanism and permits us to predict new self-ordered QWR SL structures.

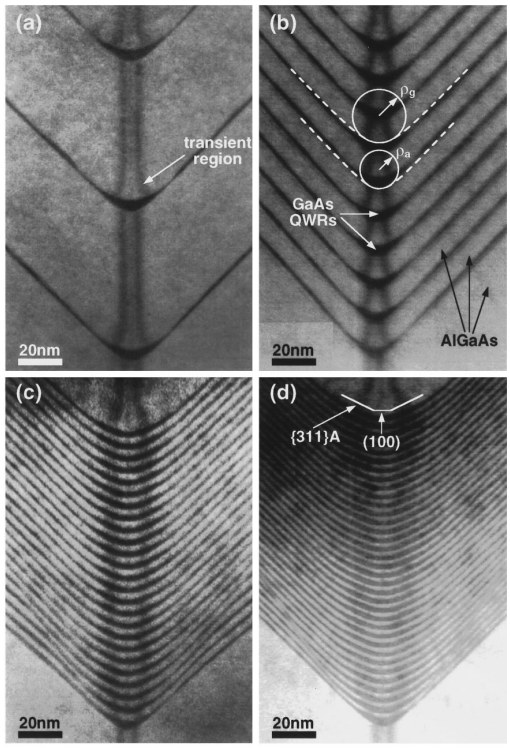

FIG. 1. TEM cross sections of (a) part of a multiple GaAs/$Al_{0.45}Ga_{0.55}As$ QWR structure (1.8 nm/60 nm); (b)–(d), 140-nm-thick GaAs/$Al_{0.45}Ga_{0.55}As$ QWR SL's with $t_g = 1.8$ nm and $t_a = 11.6$, 3.9, and 2.2 nm, respectively. $T_s = 650\,^{\circ}C$ for all samples.

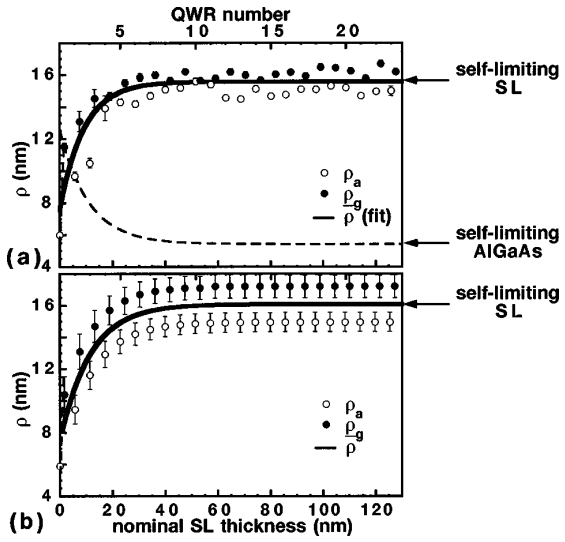

FIG. 2. (a) Evolution of the radius of curvature at the GaAs/$Al_xGa_{1-x}As$ and $Al_xGa_{1-x}As$/GaAs interfaces for the structure in Fig. 1(c). The solid line is a fit of the average radius for each SL period, the dashed line corresponds to a full recovery of ρ that would be obtained with a growth of a thick $Al_xGa_{1-x}As$ layer after the first GaAs layer. (b) Simulated evolution of the radius of curvature for the QWR-SL of Fig. 2(a).

Growth was performed in a horizontal OMCVD reactor equipped with a rotating susceptor plate at a total pressure of 20 mbar. The substrates consisted of undoped (100)-GaAs wafers, patterned along the [011] orientation with a 3-μm-pitch V-groove array.[19] We used trimethylgallium (partial pressure = 1.52 μbar), trimethylaluminum (0.47 μbar), and arsine (0.33 mbar) as precursor sources, with H_2 as a carrier gas, at a total flow of 6 l/min. The nominal growth rates were 0.3 nm/s for GaAs and 0.55 nm/s for $Al_{0.45}Ga_{0.55}As$, as measured on a planar (100) reference sample. Several samples were grown at a substrate temperature of 650 °C, all consisting of a ~350-nm-thick large period (20 nm/25 nm) GaAs/$Al_{0.45}Ga_{0.55}As$ buffer SL, a 150-nm-thick $Al_{0.45}Ga_{0.55}As$ barrier, a 140-nm-thick GaAs/$Al_{0.45}Ga_{0.55}As$ SL, and a 100-nm-thick $Al_{0.45}Ga_{0.55}As$ upper barrier. The thicknesses of the SL layers were $t_g = 1.8$ nm for GaAs and $t_a = 60$, 11.6, 7.8, 3.9, and 2.2 nm for $Al_xGa_{1-x}As$ for the different samples (subscripts g and a denote GaAs and $Al_xGa_{1-x}As$, respectively). All the nominal thicknesses given here were measured on a planar (100) reference sample. The number of SL periods was adjusted from sample to sample (10 to 30 periods), to keep the total SL thickness constant.

Figure 1 shows dark field transmission electron microscopy (TEM) cross sections of four of the samples, with $t_a = 60$, 11.6, 3.9, and 2.2 nm. In all cases, the first GaAs QWR grows on a self-limiting $Al_{0.45}Ga_{0.55}As$ V groove profile. In fact, the kinetically limited nature of the low-pressure OMCVD growth yields a self-limiting groove shape characterized by a set of (100) and {311}A nm-size facets.[19] It is useful, however, to represent the surface profile in terms of the radius of curvature ρ (see Fig. 1), defined as the radius of the circle that is tangent to the hyperbola approximating the surface profile[22] [see Fig. 1(b)]. For the self-limiting $Al_{0.45}Ga_{0.55}As$ groove of Fig. 1, $\rho_a^{sl} = 5.9 \pm 0.4$ nm. This value increases to 10.5 ± 0.9 nm after the growth of the first GaAs QWR. When t_a is well above the minimal thickness (~20–30 nm in this case) needed for a full recovery of the $Al_xGa_{1-x}As$ self-limiting profile, as for the sample of Fig. 1(a), all the vertically stacked QWR's are identical to the bottom one (within ~5% size fluctuations due to pattern and growth rate nonuniformities). In the QWR SL's of Figs. 1(b)–1(d), on the other hand, t_a is smaller than the recovery thickness, and therefore ρ just below the second GaAs crescent is larger than ρ_a^{sl}. However, after a transient expansion in the first 20 nm of the SL structure, it is seen that the groove profile reaches a stable shape, with the groove width increasing as t_a is reduced.

The evolution of the surface profile during the SL growth is summarized quantitatively in Fig. 2(a), which shows the measured values of ρ at the lower (ρ_a, open symbols) and the upper (ρ_g, filled symbols) interfaces of each GaAs QWR for the sample of Fig. 1(c), as a function of the nominal growth thickness and QWR number. After the initial widening of the groove, due to the deposition of the first QWR, the profile narrows down again upon deposition of $Al_xGa_{1-x}As$.[22] However, deposition of a second wire after only 3.9 nm of $Al_xGa_{1-x}As$ widens further the profile. This overall increase of ρ during a SL period saturates after about four periods, resulting in a new self-limiting profile. The mechanism underlying its formation consists of a widening during the wire deposition (ρ_g), balanced by an (incomplete) recovery of the $Al_xGa_{1-x}As$ profile during the subsequent deposition of the barrier layer (ρ_a). This sequence can be repeated indefinitely, yielding a stable average profile. The self-limiting average radius $\bar{\rho}_{SL} = (\bar{\rho}_a + \bar{\rho}_g)/2$, as can be seen in the plot, is constant within $\pm 2\%$ ($\bar{\rho}_{SL} = 15.6 \pm 0.3$ nm, solid line). The remaining fluctuations in $\bar{\rho}_{SL}$ are probably due to small variations in the nominal growth rate, and

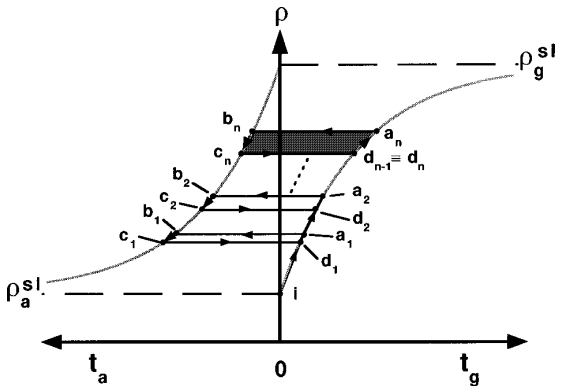

FIG. 3. Schematic representation of the curvature evolution during SL growth in the first, second, and nth period. Changes of curvature during GaAs and $Al_xGa_{1-x}As$ growth take place by following the curvature recovery curves of the material (gray lines), towards self-limiting GaAs and $Al_xGa_{1-x}As$ values (long-dashed lines).

lithography-related nonuniformities at the bottom of the groove.[23]

The formation of the stable QWR-SL phase can be understood in terms of the self-limiting growth features of ''thick'' GaAs and $Al_xGa_{1-x}As$ layers at the bottom of the V groove. Starting from an initial radius of curvature ρ_i at the bottom of the groove, ρ is found to recover exponentially to its self-limiting value ρ^{sl}:

$$\rho(t)=\rho^{sl}+(\rho_i-\rho^{sl})\exp(-t/\tau), \tag{1}$$

where t is the nominal grown thickness (proportional to the growth time) and τ is a characteristic recovery thickness.[22,23] Similar expressions hold for GaAs and $Al_xGa_{1-x}As$ growth, with parameters τ and ρ^{sl} depending on the Al mole fraction, growth temperature, and other growth parameters.[24] The evolution for the case of GaAs ($Al_xGa_{1-x}As$) growth starting from a self-limiting $Al_xGa_{1-x}As$ (GaAs) profile is shown by the gray curves in Fig. 3. To obtain the evolution of ρ for a GaAs/$Al_xGa_{1-x}As$ QWR-SL structure, we apply Eq. (1) repeatedly, obtaining the radius of curvature at the upper GaAs and $Al_xGa_{1-x}As$ surfaces of the nth SL period, respectively, as

$$\rho_{g,n}=\rho_a^{sl}+(\rho_g^{sl}-\rho_a^{sl})\exp(t_a/2\tau_a)\{1-\exp[-n(t_g/\tau_g+t_a/\tau_a)]\}\sinh(t_g/2\tau_g)/\sinh(t_g/2\tau_g+t_a/2\tau_a),$$

$$\rho_{a,n}=\rho_a^{sl}+(\rho_g^{sl}-\rho_a^{sl})\exp(-t_a/2\tau_a)\{1-\exp[-n(t_g/\tau_g+t_a/\tau_a)]\}\sinh(t_g/2\tau_g)/\sinh(t_g/2\tau_g+t_a/2\tau_a). \tag{2}$$

The self-limiting superlattice surface curvatures are obtained by setting $n\to\infty$ in Eq. (2), which yields

$$\rho_g^{SL}=\rho_g^{sl}+(\rho_a^{sl}-\rho_g^{sl})\exp(-t_g/2\tau_g)\times\sinh(t_a/2\tau_a)/\sinh(t_g/2\tau_g+t_a/2\tau_a)$$

$$\rho_a^{SL}=\rho_a^{sl}+(\rho_g^{sl}-\rho_a^{sl})\exp(-t_a/2\tau_a)\times\sinh(t_g/2\tau_g)/\sinh(t_g/2\tau_g+t_a/2\tau_a).$$

The average self-limiting radius and the difference between the GaAs and $Al_xGa_{1-x}As$ radii are given by

$$\overline{\rho}_{SL}=\frac{\rho_a^{\infty}+\rho_g^{\infty}}{2}=\frac{\rho_a^{sl}+\rho_g^{sl}}{2}+\frac{\rho_g^{sl}-\rho_a^{sl}}{2}\times\sinh(t_g/2\tau_g-t_a/2\tau_a)/\sinh(t_g/2\tau_g+t_a/2\tau_a),$$

$$\Delta\rho_{SL}=\rho_g^{\infty}-\rho_a^{\infty}=2(\rho_g^{sl}-\rho_a^{sl})\sinh(t_g/2\tau_g)\times\sinh(t_a/2t_a)/\sinh(t_g/2\tau_g+t_a/2\tau_a). \tag{3}$$

The evolution of ρ_g and ρ_a after each SL period is illustrated in Fig. 3. The SL profile starts evolving from the value ρ_a^{sl} (point i) along the GaAs recovery curve, and after the first GaAs layer it reaches the value $\rho_{g,l}$ (point a_l) determined by Eq. (1). This value, shifted horizontally onto the $Al_xGa_{1-x}As$ recovery curve (point b_1), represents the starting point of the evolution during $Al_xGa_{1-x}As$ deposition. After completing the $Al_xGa_{1-x}As$ layer, ρ decreases to the value $\rho_{a,1}$ (point c_1) that is traced back to the GaAs curve for convenience (point d_1). Since $\rho_{a,1}>\rho_a^{sl}$ the deposition of the first full SL period (contour i-a_1-b_1-c_1-d_1) brings an overall widening of the profile. This construction is repeated for the second period (contour d_1-a_2-b_2-c_2-d_2), after which the profile is characterized by $\rho_{a,2}>\rho_{a,1}$. The difference between the initial and final profile in each period tends, however, to decrease at each period, until $\rho_{a,n}=\rho_{a,n-1}$ (contour d_{n-1}-a_n-b_n-c_n-d_n, filled area in Fig. 3). At this point, growth of a full SL period forms a closed loop in the (ρ,t) plan that can be repeated *ad infinitum*.[25]

With the construction of Fig. 3, it is possible to predict and design the profile of a QWR SL structure once the recovery curves of the materials composing the individual SL layers are established. For example, one can select a desired set of values of $\overline{\rho}_{SL}$ and $\Delta\rho_{SL}$ (provided that $\overline{\rho}_{SL}-\Delta\rho_{SL}/2>\rho_a^{sl}$ and $\overline{\rho}_{SL}+\Delta\rho_{SL}/2<\rho_g^{sl}$) and construct on Fig. 3 a closed loop with $\rho_{g,a}^{SL}=\overline{\rho}_{SL}\pm\Delta\rho_{SL}/2$ that will define univocally a pair of values of t_a and t_g, yielding such a closed loop. This graphic procedure is, of course, equivalent to solving the system of Eqs. (3) for t_a and t_g.

Figure 2(b) shows $\rho_{g,n}$ and $\rho_{a,n}$ obtained with Eq. (2), as a function of the total (nominal) thickness and QWR number, for the SL of Fig. 2(a). The recovery curves were obtained from TEM cross-sectional data of growth studies for thick GaAs and $Al_xGa_{1-x}As$ layers. As for the measured profiles of Fig. 2(a), both $\rho_{g,n}$ and $\rho_{a,n}$ stabilize to values intermediate to ρ_a^{sl} and ρ_g^{sl} after an initial transient. The average radius $\overline{\rho}_{SL}$ thus obtained is 16.1 ± 0.5 nm (fitted line), in very good agreement with the experimental value. By relating the size variations of the facets at the bottom of the groove to their relative growth rates, the model is also capable of predicting accurately the growth rates of the different layers.

In the limit of a short-period QWR SL, i.e., $t_a\ll\tau_a$, $t_g\ll\tau_g$, Eq. (3) can be written as

$$\overline{\rho}_{SL}=\frac{\rho_a^{sl}+\rho_g^{sl}}{2}+\frac{\rho_g^{sl}-\rho_a^{sl}}{2}\frac{x\tau_a-\overline{x}(\tau_a+\tau_g)}{x\tau_a-\overline{x}(\tau_a-\tau_g)}, \tag{4}$$

where $\overline{x}=xt_a/(t_a+t_g)$ is the average SL Al mole fraction (note that $\overline{\rho}_{SL}\to\rho_g^{sl}$ for $\overline{x}\to0$, and $\overline{\rho}_{SL}\to\rho_a^{sl}$ for $\overline{x}\to x$, as expected). In Fig. 4 we plot the values of $\overline{\rho}_{SL}$ obtained experimentally (squares) and from Eq. (4) (solid line) as a function of the average Al composition in the SL at the bottom of the

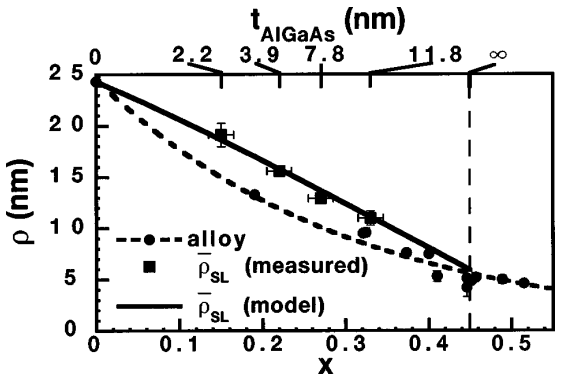

FIG. 4. Measured (squares) and calculated (solid line) mean QWR-SL radius of curvature, as a function of the average Al mole fraction in the SL, for $T_s = 650\,^{\circ}$C. Self-limiting radii of curvature of $Al_xGa_{1-x}As$ alloys are shown by circles, with a dashed line as a guide to the eye.

groove. The measured data are well reproduced by expression (4). However, the observed radius of curvature of the SL is systematically larger than the measured self-limiting radius ρ_a^{sl} for $Al_xGa_{1-x}As$ *alloys* with the same equivalent composition x grown under the same conditions (circles in Fig. 4; the corresponding dashed line is a guide to the eye). In other words, the surface curvature depends not only on the local relative abundance of the group-III species but also on the order in which they are deposited (pure $GaAs + Al_xGa_{1-x}As$, or $Al_yGa_{1-y}As$ alloy). In particular, since Eq. (4) is independent of the absolute thicknesses of the SL layers, the discrepancy above holds also in the limit of t_a, $t_g \rightarrow 0$, that would correspond to the epitaxial growth of an alloy by alternate deposition of its constituents (''digital'' alloy).

The smaller radius of curvature for the alloy case can be qualitatively explained as due to the contribution of the entropy of mixing (see, e.g., Ref. 26, p. 52) of the two group-III components to the surface diffusion fluxes of adatoms, which determine the size of ρ. As we will discuss in a forthcoming paper,[20] the realization of self-limited growth in the case of a binary can be interpreted as an equilibrium state between the effects of growth rate anisotropy on the different planes composing the groove (that would tend to sharpen up the bottom) and of adatom migration towards the bottom, due to curvature-related differences of the surface chemical potential[27] (that would tend to broaden it). However, in the case of a ternary alloy, the excess Ga concentration at the bottom of the groove[28] yields a different entropy of mixing in that region, and hence a lower (higher) surface chemical potential for Al (Ga). This, in turn, results in additional surface fluxes that tend to reduce the Ga concentration at the bottom of the groove so as to counteract the segregation due to curvature-induced effects. As a consequence, the self-limiting groove profile is narrower than what it would be in the absence of the entropy term. For the case of separate deposition of the binary compounds, on the other hand, the entropy term is absent and the growth rate and curvature are determined only by surface fluxes arising from the local surface curvature. A similar effect should hold when comparing the deposition of an alloy with the equivalent binary and ternary SL layers.

In summary, we have shown that a self-ordered phase of a QWR superlattice is formed during OMCVD on V-grooved substrates due to an exact balance of the expansion and partial recovery of the surface curvature during growth of the low band-gap and high band-gap SL layers. A simple model employing the self-limiting growth characteristics of thick layers on such curved surfaces yields quantitative understanding of the details of the resulting QWR SL structure. A similar mechanism of QWR SL formation should hold also for other nonplanar structures exhibiting a self-limiting growth behavior. The resulting SL structures exhibit better uniformity than other low-dimensional (QWR or QD) SL structures produced via different self-ordering mechanisms, such as strain induced SK or tilted SL structures, indicating a stronger driving force of the grown species to their nucleation sites in the case of the nonplanar growth. These structures should thus be useful for studying the coupling and tunneling phenomena in SL's of 1D systems.[29]

This work was partially supported by the Fonds National Suisse de la Recherche Scientifique. We wish to thank A. Rudra for helping with the OMCVD growth.

*Present address: Department of Solid State Physics, Lund University, Box 118, S-221 00 Lund, Sweden.

[1] E. E. Mendez, F. Agulló-Rueda, and J. M. Hong, Phys. Rev. Lett. **60**, 2426 (1988).
[2] G. V. Plessen and P. Thomas, Phys. Rev. B **45**, 9185 (1992).
[3] J. Feldmann *et al.*, Phys. Rev. B **46**, 7252 (1992).
[4] K. Leo, Solid State Commun. **84**, 943 (1992).
[5] C. Waschke *et al.*, Phys. Rev. Lett. **70**, 3319 (1993).
[6] T. Fukui and H. Saito, Appl. Phys. Lett. **50**, 824 (1987).
[7] M. Tsuchiya, P. M. Petroff, and L. A. Coldren, Appl. Phys. Lett. **54**, 1690 (1989).
[8] M. S. Miller *et al.*, Phys. Rev. Lett. **68**, 3464 (1992).
[9] C. Giannini *et al.*, Phys. Rev. B **55**, 5276 (1997).
[10] Q. Xie *et al.*, Phys. Rev. Lett. **75**, 2542 (1995).
[11] J. Tersoff, C. Teichert, and M. G. Lagally, Phys. Rev. Lett. **76**, 1675 (1996).
[12] C. Teichert *et al.*, Phys. Rev. B **53**, 16 334 (1996).
[13] G. Solomon *et al.*, Phys. Rev. Lett. **76**, 952 (1996).
[14] M. K. Zundel *et al.*, Appl. Phys. Lett. **71**, 2972 (1997).
[15] A. Krost *et al.*, Appl. Phys. Lett. **68**, 785 (1996).
[16] A. A. Darhuber *et al.*, Phys. Rev. B **55**, 15 652 (1997).
[17] A. C. Chen *et al.*, Appl. Phys. Lett. **62**, 1359 (1993).
[18] E. Kapon, D. M. Hwang, and R. Bhat, Phys. Rev. Lett. **63**, 430 (1989).
[19] A. Gustafsson *et al.*, Appl. Phys. Lett. **67**, 3673 (1995).
[20] G. Biasiol and E. Kapon (unpublished).
[21] E. Kapon *et al.*, NATO ASI Ser., Ser. E **298**, 291 (1995).
[22] E. Kapon *et al.*, Solid-State Electron. **40**, 815 (1996).
[23] G. Biasiol *et al.*, Appl. Phys. Lett. **71**, 1831 (1997).
[24] Note that the form of the evolution of ρ, defined by τ, is independent of the initial value. This was verified experimentally on $Al_xGa_{1-x}As$ layers grown under identical conditions on GaAs layers of different thicknesses, defining, therefore, different initial profiles.
[25] Of course, after growth of a sufficiently thick structure (of a thickness comparable to the depth of the initial groove), the structure planarizes, due to the expansion of the top of the mesas. A periodic recovery of the surface profile as in Fig. 3 occurs only at the bottom of the groove before planarization is achieved.
[26] J. Y. Tsao, *Material Fundamentals of Molecular Beam Epitaxy* (Academic, Boston, 1993).
[27] W. W. Mullins, J. Appl. Phys. **28**, 333 (1957).
[28] The Al mole fraction at the bottom of the groove is lower than the nominal one, giving rise to the formation of a vertical quantum well [G. Biasiol *et al.*, Appl. Phys. Lett. **69**, 2710 (1996)], as an effect of a more efficient diffusion of Ga towards the bottom, with respect to Al.
[29] Y. Ducommun *et al.*, Physica E (to be published).